Linking NH_4^+ motion to magnetism in molecular multiferroic $(NH_4)_2[FeCl_5(H_2O)]$: A neutron vibrational spectroscopy study

W. Tian [*], L. L. Daemen, Y. Q. Cheng, Fei Li, and Jaime A. Fernandez-Baca
Neutron Scattering Division, Oak Ridge National Laboratory, Oak Ridge, Tennessee 37831, USA

We present a neutron vibrational spectroscopy study to investigate the influence of NH_4^+ motion on the magnetism in $[(NH_4)_{1-x}K_x]_2[FeCl_5(H_2O)]$. The parent compounds, $(NH_4)_2[FeCl_5(H_2O)]$ ($x = 0$) and $K_2[FeCl_5(H_2O)]$ ($x = 1$) are isostructural at room temperature, yet displaying drastically different magnetic and multiferroic behavior. $K_2[FeCl_5(H_2O)]$ is nonmultiferroic with type-A collinear antiferromagnetic structure below $T_N \approx 14.06$ K, whereas $(NH_4)_2[FeCl_5(H_2O)]$ is a type-II multiferroic with incommensurate cycloidal spin structure below $T_{FE} \approx 6.8$ K. A recent study of the dielectric, structure, and magnetic properties in the mixed $[(NH_4)_{1-x}K_x]_2[FeCl_5(H_2O)]$ shows that a small amount of potassium substitution to replace NH_4^+ transforms the spin structure from incommensurate cycloidal ($x \leqslant 0.06$) into commensurate collinear antiferromagnetic ($x \geqslant 0.15$), indicating NH_4^+ is essential to the emergent phenomena observed in this molecular multiferroic compound. Our vibrational spectroscopy study reveals that NH_4^+ libration and torsion motion exhibit substantial temperature dependence at low temperatures. The intensity of NH_4^+ libration and torsion modes increases slightly at 5 K in comparison with data at 25 K behaving like a magnon, indicating that they are coupled to the magnetism in $(NH_4)_2[FeCl_5(H_2O)]$. Comparing data of $x = 0$, 0.06, 0.09, and 0.15 samples further illustrates that the strength of the increased signal in NH_4^+ libration mode is very sensitive to potassium concentration. The signal diminishes quickly with increasing potassium concentration and vanishes in the $x = 0.15$ sample corresponding to the magnetic structure change for $x \geqslant 0.15$. The results directly link the anomalous behavior in NH_4^+ libration motion to the magnetism in $[(NH_4)_{1-x}K_x]_2[FeCl_5(H_2O)]$, providing new insights into the crucial role NH_4^+ plays in the coupled phenomena in $(NH_4)_2[FeCl_5(H_2O)]$. The unique information opens a new door to go through in searching for new multifunctional materials by incorporation of NH_4 via a material-by-design approach.

I. INTRODUCTION

Spin-driven multiferroics (also referred to as type-II multiferroics) exhibit a strong magnetoelectric (ME) effect owing to the direct coupling between magnetism and electric polarization [1,2]. This class of materials possesses great potential for technological applications in multifunctional devices, igniting enormous studies over the last couple of decades to unveil the underlying ME coupling mechanism. Type-II multiferroic materials also represent a unique branch of modern research hosting emergent phenomena arising from the intricate interplay between lattice, spin, charge, and orbital degrees of freedom. However, natural single-phase spin-driven multiferroics are rare, and most known systems are transition-metal oxides, such as TbMnO3 [3–9], MnWO4 [10], Ni3V2O8 [11], CuO [12], LiCuVO4 [13], and CaCoMnO3 [14]. Recently, $(NH_4)_2[FeCl_5(H_2O)]$ is identified to be one of the first molecule-based magnets exhibiting a type-II multiferroic behavior [15]. Thermodynamic properties of this ammonium-containing molecular compound manifest complex multiferroic properties and rich physics, which are highly tailorable by external stimuli, providing a fascinating platform for manipulating and crosscontrolling the ME coupling effect.

$(NH_4)_2[FeCl_5(H_2O)]$ belongs to the erythrosiderites family with chemical formula $A_2[FeCl_5(H_2O)]$ (where A = K, Rb, NH4) [16–19]. The crystal structure is orthorhombic (space group *Pnma*) at room temperature with Fe^{3+} magnetic ion coordinated by five Cl^- ions and a water molecule H_2O [18]. The (K^+, Rb^+) cations or NH_4^+ tetrahedra are isolated from the slightly distorted $[FeCl_5(H_2O)]^{2-}$ octahedra as depicted in Figs. 1(a) and 1(b). Although the unusual magnetic behavior of $(NH_4)_2[FeCl_5(H_2O)]$ was first reported in the 1970's [16], the magnetic structure remained unknown due to the large amount of hydrogen atoms (40 H atoms per unit cell) in this compound. It was only recently that the magnetic structure was determined by neutron diffraction studies [20,21]. Three transitions were clearly observed in the specific heat data of $(NH_4)_2[FeCl_5(H_2O)]$ upon cooling: a structural transition at $T_s \approx 79$ K, and two successive magnetic transitions at $T_N \approx 7.3$ K and $T_{FE} \approx 6.8$ K, with the latter accompanied by spontaneous ferroelectric polarization [15]. Neutron diffraction study reveals that the structural transition at T_s can be attributed to a disorder-order transition of the NH_4 group with crystal symmetry changing from orthorhombic *Pnma* to monoclinic $P112_1/a$ [Fig. 1(b)], whereas the magnetic structure is determined to be a collinear sinusoidal between $T_{FE} < T < T_N$ [21] and an incommensurate cycloidal spiral below T_{FE} [Fig. 1(d)] [20]. The electric polarization is realized via two magnetic transitions characteristic of a type-II
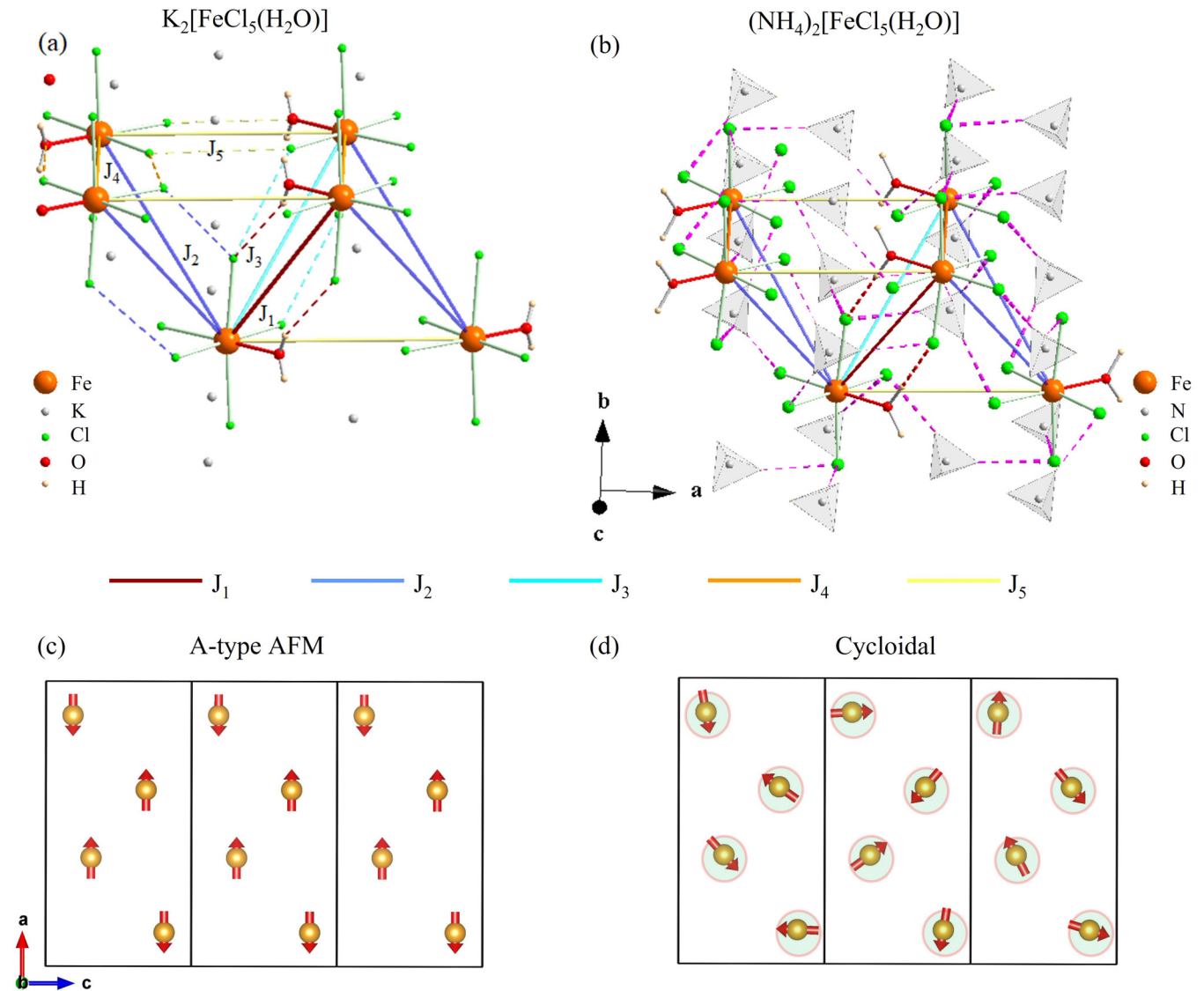
[*] Contact author: wt6@ornl.gov

FIG. 1. Crystal and magnetic structure of $K_2[FeCl_5(H_2O)]$ and $(NH_4)_2[FeCl_5(H_2O)]$. (a) Crystal structure of $K_2[FeCl_5(H_2O)]$ at 2 K. The magnetic exchange interactions up to the fifth-nearest neighbors (J_1 to J_5) are shown. The solid lines represent interactions connecting the Fe^{3+} - Fe^{3+} ions, whereas the dotted lines illustrate the "parallel edge" sharing double superexchange pathways. The magnetic interaction of J_1 are mediated through Fe-O-H...Cl-Fe involving hydrogen bonding in both superexchange pathways; J_2 and J_3 exchange interactions are mediated through Fe-Cl...Cl-Fe in both superexchange pathways with no hydrogen and oxygen atom involved; whereas for J_4 and J_5, the interaction is mediated through Fe-O...Cl-Fe and Fe-Cl...Cl-Fe with one superexchange pathway containing an oxygen atom, without hydrogen bonding [19]. (b) Crystal structure of $(NH_4)_2[FeCl_5(H_2O)]$ at 2 K with ordered NH_4^+ tetrahedra [20]. The dominant magnetic interactions J_1 to J_5 are plotted same as in $K_2[FeCl_5(H_2O)]$. For clarity, the Fe-O-H...Cl-Fe, Fe-O...Cl-Fe, and Fe-Cl...Cl-Fe type double superexchange pathways are not shown. Instead, the N-H...Cl, O-H...Cl type hydrogen bonds are shown in purple dashed lines to illustrate the extended complex hydrogen-bonding network mediated through NH_4. (c) A-type antiferromagnetic magnetic structure of $K_2[FeCl_5(H_2O)]$ viewed along the *b* axis. (d) Incommensurate cycloidal-spiral spin structure of $(NH_4)_2[FeCl_5(H_2O)]$ at 2 K viewed along the *b* axis. Three unit cells along the *c* axis are plotted, and only magnetic Fe^{3+} ions are shown in (c) and (d) for clarity.

multiferroic with inverse Dzyaloshinsky–Moriya (IDM) interactions [3,10,11]. Even-order harmonics associated with the incommensurate wave vector of the cycloidal structure were observed below T_{FE}, indicating that the onset of the electric polarization is accompanied by a lattice modulation and mediated by spin-lattice coupling [21]. Moreover, $(NH_4)_2[FeCl_5(H_2O)]$ exhibits exotic phenomena intriguing among type-II multiferroics. The ME effect is very sensitive to the magnetic field and pressure: applying a modest magnetic field (up to 6 T) along the *a* axis or *c* axis induces transitions to

distinct magnetic and ferroelectric phases [15]; applying modest hydrostatic pressure (up to 1 GPa) induces multiple exotic metastable phases, and a reentrant-type behavior is observed [22]. Based on the determined magnetic structures, a magnetic field-induced change of ME coupling mechanism from the spin-current IDM model at low fields to the spin-dependent p-d hybridization model at high fields has been proposed [23,24]. Furthermore, there exists a regime in the B vs T phase diagram (B ∥ a) where it seems that a direct transition from a paramagnetic/nonferroelectric (PM/Non-FE) phase to an

TABLE I. The magnetic interactions up to the fifth-nearest neighbors J_1 to J_5, and the single-ion anisotropy parameter D determined by fitting the measured magnetic spectrum using a linear spin-wave theory model as described in Ref. [32] for (ND$_4$)$_2$[FeCl$_5$(D$_2$O)] (0 T) and Ref. [19] for K$_2$[FeCl$_5$(D$_2$O)], respectively.

Compound	J_1 (meV)	J_2 (meV)	J_3 (meV)	J_4 (meV)	J_5 (meV)	D (meV)
(ND$_4$)$_2$[FeCl$_5$(D$_2$O)] (0 T)	0.177(10)	0.064(5)	0.029(7)	0.056	0.035	0.015(7)
(ND$_4$)$_2$[FeCl$_5$(D$_2$O)] (6 T)	0.181(13)	0.051(3)	0.033(4)	0.055 (3)	0.039(7)	0.014(6)
K$_2$[FeCl$_5$(D$_2$O)] (0 T)	0.113(3)	0.037(1)	0.032(3)	0.023(2)	0.025(2)	0.0146

antiferromagnetic/ferroelectric (AFM/FE) phase occurs [15]. Such a direct transition is exceptionally rare, and it would require the involvement of two different order parameters concurrently [25–27]. Our prior neutron diffraction study reveals that the direct transition can be accounted for by the coexistence of incommensurate and commensurate orders [28], and the phase coexistence was further investigated in Ref. [29] recently.

The intriguing properties observed in (NH$_4$)$_2$[FeCl$_5$(H$_2$O)] are in stark contrast to its counterpart K$_2$[FeCl$_5$(H$_2$O)] from the same family. For K$_2$[FeCl$_5$(H$_2$O)], a single magnetic phase transition was observed at $T_N \approx 14.06$ K. As shown in Fig. 1(a), the crystal structure remains orthorhombic down to 2 K [18] with a = 13.439 Å, b = 9.598 Å, c = 6.98 Å, and $\alpha = \beta = \gamma = 90°$. The magnetic ground state is a type-A collinear antiferromagnetic spin structure with moment along the a axis as depicted in Fig. 1(c). The linear magnetoelectric effect was observed but the electric polarization can only be induced below 14.06 K under applied magnetic fields; hence, K$_2$[FeCl$_5$(H$_2$O)] is nonmultiferroic [30]. The prime magnetic interactions (J_1 to J_5 up to the fifth-nearest neighbors) between Fe^{3+} ions are mediated via Fe-O-H...Cl-Fe, Fe-O...Cl-Fe, and Fe-Cl...Cl-Fe type "parallel edge" sharing double superexchange pathways as illustrated in Fig. 1(a). The microscopic magnetic interactions in K$_2$[FeCl$_5$(H$_2$O)] were determined by inelastic neutron scattering and DFT studies using a Heisenberg spin model including a single ion anisotropy term [19]. The obtained value of the magnetic interactions are listed in Table I, where J_1 is the strongest interaction involving hydrogen bonding, all other interactions (J_2 to J_5) are weaker and are of the same order of magnitude [31].

On the other hand, while the crystal structure of (NH$_4$)$_2$[FeCl$_5$(H$_2$O)] is orthorhombic at room temperature, the symmetry of the system changes to monoclinic below 79 K due to a disorder-order transition induced by the NH$_4$ group [lattice parameters at 2 K: a = 13.5019 (Å), b = 9.9578 (Å), c= 6.9049 (Å), $\alpha = 90°$, $\beta = 90°$, and $\gamma = 90.109°$] resulting in a ~0.1° change in γ angle [20]. As shown in Fig. 1(b), the subtle structural transition has minor effect to the local environment of Fe^{3+} magnetic ions in (NH$_4$)$_2$[FeCl$_5$(H$_2$O)]. The [FeCl$_5$(H$_2$O)]$^{2-}$ local octahedra distortion is increased slightly, and the prime magnetic interactions (J_1 to J_5) are mediated by the double superexchange pathways, same as K$_2$[FeCl$_5$(H$_2$O)]. Inelastic neutron scattering studies of (NH$_4$)$_2$[FeCl$_5$(H$_2$O)] [32] reveal that although the zero-field and high-field multiferroic phases involve different ME coupling mechanisms, the spin dynamics of both phases can be well described by a Heisenberg Hamiltonian with easy-plane anisotropy similar to the linear

spin wave model used in fitting the magnetic spectrum of K$_2$[FeCl$_5$(H$_2$O)] [19]. The obtained value of the magnetic interactions at zero field and 6 T are listed in Table I. Comparing with K$_2$[FeCl$_5$(H$_2$O)], the exchange interactions J_1, J_2, J_4, and J_5 are stronger in (NH$_4$)$_2$[FeCl$_5$(H$_2$O)], except for J_3 which becomes weaker, consistent with the reported distances (Å) in Ref. [33] (Table S1 in the Supplemental Material) between the ligand atoms involved in the double superexchange pathways in K$_2$[FeCl$_5$(H$_2$O)] and (NH$_4$)$_2$[FeCl$_5$(H$_2$O)]. By replacing K^+ with NH_4^+, the J_1, J_2, J_4, and J_5 exchange pathways become shorter (stronger interaction), except for J_3 which has longer pathways in (weaker interaction) (NH$_4$)$_2$[FeCl$_5$(H$_2$O)]. The inelastic neutron scattering studies of (NH$_4$)$_2$[FeCl$_5$(H$_2$O)] [32] further reveals that J_2 and J_4 are roughly the same size, forming a buckled triangular-lattice plane coupled via J_1, J_3, and J_5 which gives rise to enhanced magnetic frustration in this compound. This implies that the enhanced magnetic frustration and the intriguing multiferroic properties in (NH$_4$)$_2$[FeCl$_5$(H$_2$O)] are directly linked to the incorporation of NH$_4^+$ ions. A study of mixed [(NH$_4$)$_{1-x}$K$_x$]$_2$[FeCl$_5$(H$_2$O)] [34] reveals that even a small amount of potassium substitution would release the magnetic frustration and switch the spin structure from incommensurate cycloidal ($x \leqslant 0.06$) into A-type collinear antiferromagnetic ($x \geqslant 0.15$). An earlier Mössbauer spectroscopy study shows constant Fe quadrupole splitting Δ for K$_2$[FeCl$_5$(H$_2$O)], whereas Δ in (NH$_4$)$_2$[FeCl$_5$(H$_2$O)] depicts strong temperature dependence which was explained in terms of thermally activated reorientation of the NH$_4^+$ ions. Low temperature Mössbauer spectra at $T = 4.2$ K also shows anomalies in (NH$_4$)$_2$[FeCl$_5$(H$_2$O)] in comparison with K$_2$[FeCl$_5$(H$_2$O)], providing indirect evidence that NH$_4^+$ plays a critical role in the magnetic property of (NH$_4$)$_2$[FeCl$_5$(H$_2$O)] [35]. In this paper, we report a neutron vibrational spectroscopy study of [(NH$_4$)$_{1-x}$K$_x$]$_2$[FeCl$_5$(H$_2$O)] series that provides insights into the crucial role NH$_4^+$ plays in the emerging phenomena in (NH$_4$)$_2$[FeCl$_5$(H$_2$O)].

II. EXPERIMENTAL DETAILS

Vibrational spectroscopy can provide insightful information at the molecular level. To investigate how NH$_4^+$ incorporation and its motion affect the magnetism in (NH$_4$)$_2$[FeCl$_5$(H$_2$O)], we performed an inelastic neutron scattering (INS) experiment to study the NH$_4$ motions in mixed [(NH$_4$)$_{1-x}$K$_x$]$_2$[FeCl$_5$(H$_2$O)] using the VISION neutron spectrometer at the Spallation Neutron Source (SNS) at Oak Ridge National Laboratory (ORNL). VISION is designed to study the vibrational dynamics of atoms in molecules and solids. The instrument is optimized to measure molecular
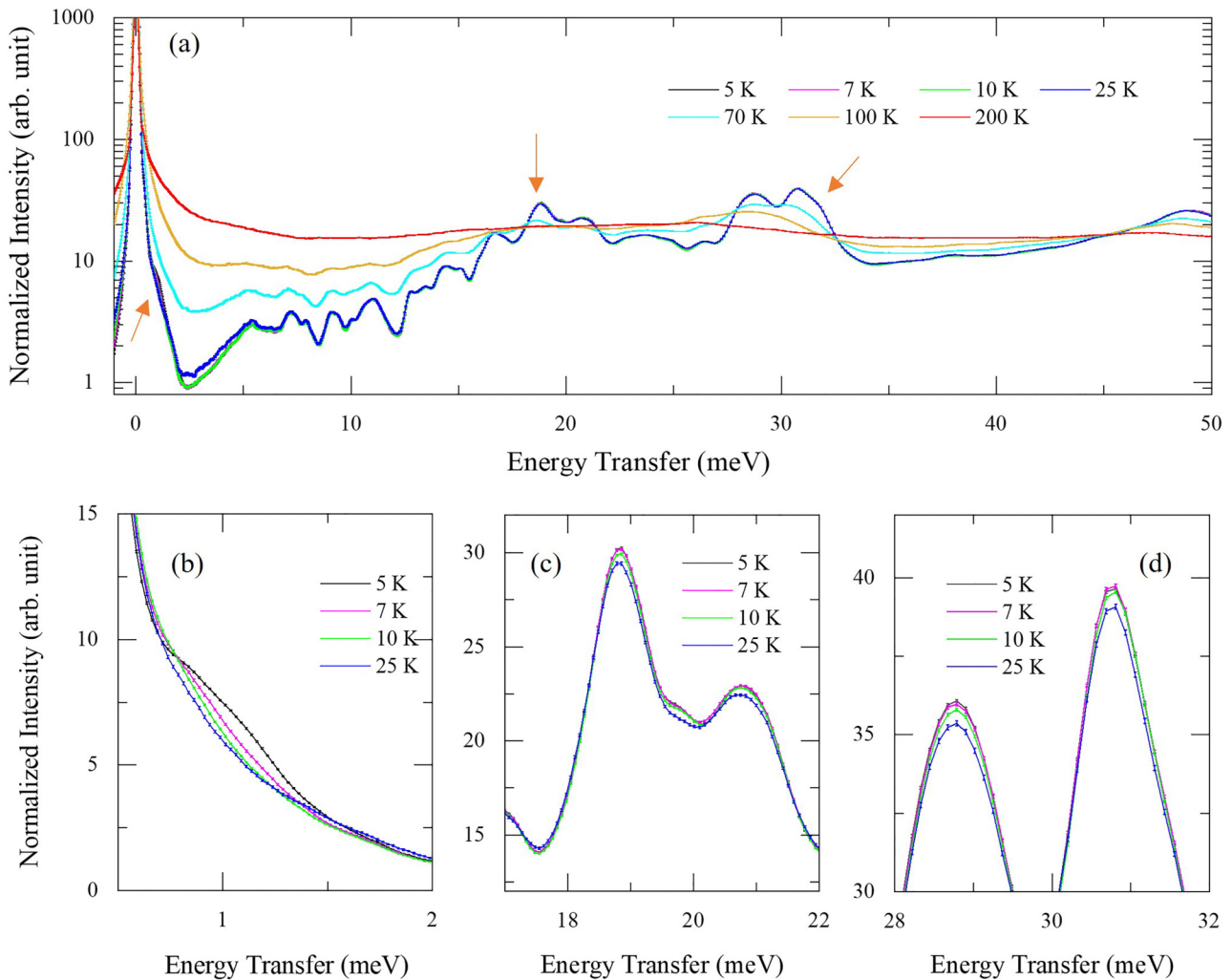
FIG. 2. (a) Vibrational spectroscopy spectra measured at selected temperatures, T = 5 K, 7 K, 10 K, 25 K, 70 K, 100 K, and 200 K on $(NH_4)_2[FeCl_5(H_2O)]$ powder. The normalized intensities are plotted on a logarithmic scale. The arrows depict the three enlarged regions plotted in (b), (c), and (d), respectively. Temperature dependence of (b) magnetic excitation around ~1 meV; (c) NH_4 libration modes between 18 to 22 meV; (d) NH_4 torsion modes between 28 to 32 meV for T = 5 K, 7 K, 10 K, and 25 K.

vibrations over a broad energy range (−2–1000 meV) at high resolutions by employing indirect-geometry spectroscopy. $[(NH_4)_{1-x}K_x]_2[FeCl_5(H_2O)]$ polycrystalline samples, $x = 0$, 0.06, 0.09, and 0.15, were obtained from grinding tiny crystals grown from aqueous solutions with a surplus of HCl and 2:1 molar ratio between $FeCl_3$ and $[(1-x)NH_2Cl + x KCl]$ as described in Ref. [34]. Each powder sample was loaded and sealed in a vanadium can under Helium atmosphere, and a closed-cycle refrigerator was used to control the temperature between 5 K and 300 K. For each sample, data were collected at selected temperatures, T = 5 K, 7 K, 10 K, 25 K, 70 K, 100 K, and 200 K. The spectrum was normalized to the elastic peak and total measurement time by proton charge. Empty can data were subtracted as background.

III. RESULTS AND DISCUSSIONS

Figure 2 compares the vibrational spectroscopy spectra of $(NH_4)_2[FeCl_5(H_2O)]$ measured at selected temperatures between 5 K and 200 K. In order to illustrate the evolution of

intensity and spectral line shape as a function of temperature, the low energy spectra between −2 meV and 50 meV were plotted on a logarithmic scale in Fig. 2(a). At first glance, two features are clearly observed: (i) Quasielastic scattering was observed arising from low energy molecular motions at 70 K and above. The signal increases with increasing temperature. (ii) The spectral line shape changes drastically comparing data at 70 K and 100 K associated with the onset of the order-disorder transition at $T_s \approx 79$ K. The spectra are nearly featureless above 79 K, reflecting average structure due to the random orientation of NH_4^+ tetrahedron. In sharp contrast, modes appear in the spectra below 79 K and exhibit more prominent features upon cooling because NH_4^+ tetrahedra become well-ordered below the order-disorder transition. However, as we examine the low-temperature data in more detail, a few modes (depicted by the arrows) exhibit anomalous temperature dependence behavior below 25 K. The enlarged regime comparing the spectra at 5 K, 7 K, 10 K, and 25 K with energy transfer ranges of 0.7–1.3 meV, 18–22 meV, and 28–32 meV are plotted in Figs. 2(b)–2(d), respectively.

As shown in Fig. 2(b), the excitation around 0.7–1.3 meV is strongest at 5 K, and the signal becomes weaker with increasing temperature and eventually vanishes at 25 K. This excitation is identified to be magnetic in origin, consistent with our prior INS report [32]. The excitation between 18–22 meV [Fig. 2(c)] and 28–32 meV [Fig. 2(d)] are assigned to NH$_4$ libration and NH$_4$ torsion modes, respectively, based on the phonon calculations using the parameters of monoclinic structure determined at 2 K. Details of phonon calculations and peak assignment related to these modes are described in the Supplemental Material [36] (see also Refs. [37–45] therein). The INS intensities associated with NH$_4$ libration and torsion modes are expected to behave like phonons with intensity increasing with increasing temperatures. Given that the energy scale of the libration ($\sim$20 meV) and torsion ($\sim$30 meV) modes correspond to $T \sim 232$ K and $T \sim 348$ K, respectively, one wouldn't expect much change in intensity within a narrow temperature range between 5 K and 25 K. Therefore, it is quite unusual to observe that the intensity of both modes is enhanced slightly with decreasing temperature. The increased signal in NH$_4$ libration and torsion modes at 5 K in comparison with data at 25 K indicates that they are dressed by magnetic order, providing evidence of intertwining coupling between NH$_4$ libration and torsion motion and the magnetism in (NH$_4$)$_2$[FeCl$_5$(H$_2$O)].

We further investigate the increased signal in NH$_4$ libration and torsion motions, comparing data in mixed [(NH$_4$)$_{1-x}$K$_x$]$_2$[FeCl$_5$(H$_2$O)] for $x = 0$, 0.06, 0.09, and 0.15. The difference spectra of pure (NH$_4$)$_2$[FeCl$_5$(H$_2$O)] were plotted over a wide energy range in Fig. 3(a), where the data at 5 K were subtracted from data at 7 K, 10 K, and 25 K, to illustrate the excitations exhibiting substantial temperature dependence between 0 and 150 meV. Low-energy phonon populations (labeled by the black arrow) with signal increasing with increasing temperature are observed below 10 meV. In addition to the NH$_4$ libration and torsion modes around $\sim$20 meV and $\sim$30 meV, which show enhanced signal at 5 K, there is a third mode around $\sim$50 meV exhibiting similar temperature dependence behavior. Based on the phonon calculation, this excitation is identified to be the water-wagging mode. The intensity of the water-wagging mode increases with decreasing temperature between 5 K and 25 K, indicating that the water molecule also plays a role in the magnetic transitions. The animations illustrating the motions of the NH$_4$ libration, NH$_4$ torsion, and water-wagging modes are shown in the Supplemental Material [36]. We also show the enlarged regime of Fig. 3(a) between 0 meV and 15 meV in Fig. S1 in the Supplemental Material [36] to illustrate the different temperature dependence behavior of the phonon modes and low-lying magnetic excitations as depicted in Fig. 2(b).

To examine the effect of potassium substitution on the enhanced signal of NH$_4$ libration and torsion motions observed at 5 K, we compare the difference spectrum (data at 5 K were subtracted from data at 25 K) of [(NH$_4$)$_{1-x}$K$_x$]$_2$[FeCl$_5$(H$_2$O)] ($x = 0$, 0.06, 0.09, and 0.15) in Fig. 3(b). Because the molecular mass varies with increasing potassium concentration, each spectrum in Fig. 3(b) was normalized to contain the same mole of NH$_4$ for direct comparison. The difference spectrum is plotted between 10 meV and 60 meV to include all three effected modes, NH$_4$ libration, NH$_4$ torsion,
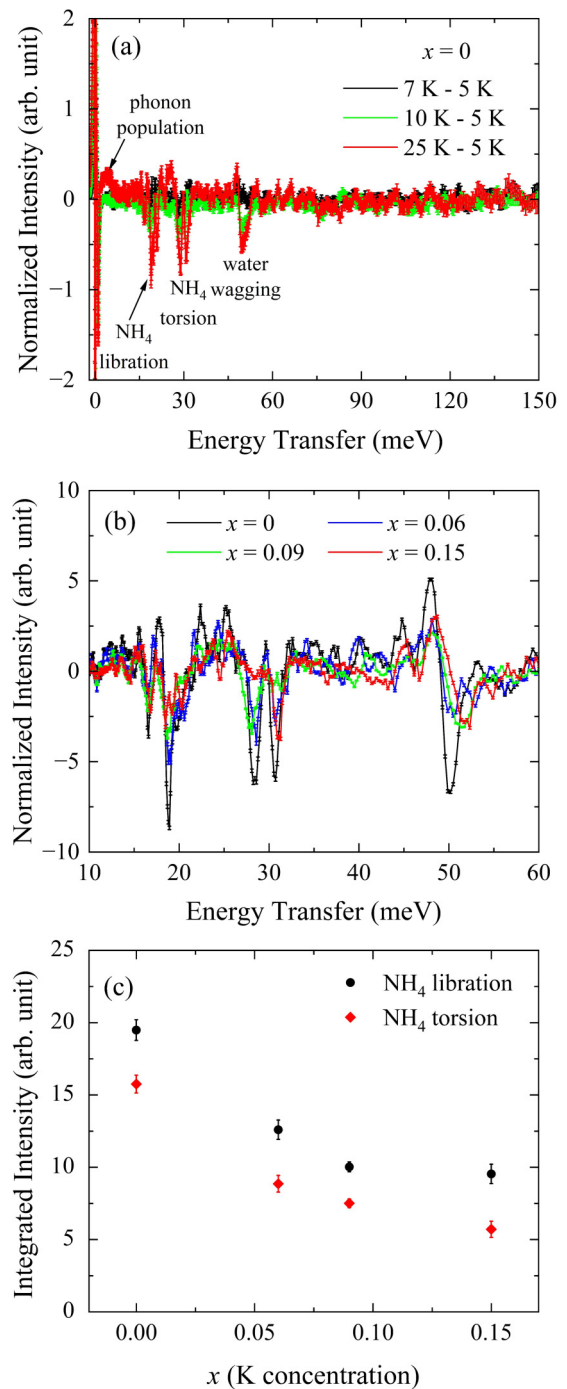

FIG. 3. (a) Difference spectra (data at 5 K were subtracted from data at 7 K, 10 K, and 25 K) of (NH$_4$)$_2$[FeCl$_5$(H$_2$O)] plotted with energy transfers up to 150 meV to illustrate the low temperature behavior of NH$_4$ libration and torsion motion. (b) Comparison between difference spectra (data at 5 K were subtracted from data at 25 K) of mixed [(NH$_4$)$_{1-x}$K$_x$]$_2$[FeCl$_5$(H$_2$O)] for $x = 0$, 0.06, 0.09, and 0.15. (c) Integrated intensity of the enhanced signal in NH$_4$ libration and NH$_4$ torsion motions as a function of potassium concentration x.

and water-wagging motions. Data shows that all three modes respond strongly with increasing potassium substitution. At first glance, the peak intensity of the enhanced signal in NH$_4$ libration drops sharply in the $x = 0.06$ sample, further

decreases in the $x = 0.09$ sample, and vanishes in the $x = 0.15$ sample corresponding to the magnetic structure change as reported in $[(NH_4)_{1-x}K_x]_2[FeCl_5(H_2O)]$ in Ref. [34], with spin structure switching from incommensurate cycloidal for $x \leqslant 0.06$ to A-type collinear antiferromagnetic for $x \geqslant 0.15$. The peak intensity of the enhanced signal in NH_4 torsion and water-wagging motions, on the other hand, do not show monotonic change with increasing potassium substitution. Given that the enhanced signal is rather weak in the difference spectrum, it is necessary to compare the integrated intensity in order to clarify the effect of potassium substitution on the enhanced signal of NH_4 libration and torsion motions. The integrated intensity of NH_4 libration and torsion motions are plotted in Fig. 3(c) as a function of potassium concentration x, where the intensity at each x are integrated over a fixed energy transfer range of 14–24 meV for NH_4 libration motions and 26–33 meV for NH_4 torsion motions, respectively. It shows both modes behave the same and the enhanced signal is suppressed upon increasing potassium substitution. The vibrational spectroscopy results hence provide experimental evidence directly linking the anomalous behavior of NH_4 libration and torsion motions to the magnetic structure change in $[(NH_4)_{1-x}K_x]_2[FeCl_5(H_2O)]$. The water-wagging mode also responds to potassium substitution strongly, similar to the NH_4 torsion mode [Fig. 3(b)]. As depicted in Figs. 1(a) and 1(b), water molecules are directly involved in the double superexchange pathways of J_1 which is the strongest magnetic interaction in $K_2[FeCl_5(H_2O)]$ and $(NH_4)_2[FeCl_5(H_2O)]$, linking the neighboring octahedra by Fe-O-H...Cl-Fe hydrogen bonds. Consequently, there is no doubt that water molecules play an important rule in the magnetism in both compounds. However, as we will discuss below, we believe that the anomalous behavior of the water-wagging motion and its strong response to potassium substitution are induced by the extended complex hydrogen-bonding network mediated through NH_4^+ in $[(NH_4)_{1-x}K_x]_2[FeCl_5(H_2O)]$.

To further explain the findings from the vibrational spectroscopy study in-depth, we compare the valid magnetic exchange pathways in $(NH_4)_2[FeCl_5(H_2O)]$ and $K_2[FeCl_5(H_2O)]$. As shown in Figs. 1(a) and (b), the significant difference between the two compounds is that there exists an extended complex hydrogen-bonding network mediated through NH_4^+ in $(NH_4)_2[FeCl_5(H_2O)]$. Therefore, in addition to the prime magnetic interactions (J_1 to J_5), the magnetic Fe^{3+} ions are also connected via additional Fe-Cl...H-N-H...Cl-Fe type magnetic exchange pathways. The magnitudes of such coupling are much weaker compared to J_1 to J_5 so that they can be neglected in describing the spin dynamics in $(NH_4)_2[FeCl_5(H_2O)]$ [32]. However, the temperature dependence measurements indicate spin-lattice coupling evidenced by the enhanced intensity in the NH_4^+

libration and torsion modes at 5 K. The study of mixed $[(NH_4)_{1-x}K_x]_2[FeCl_5(H_2O)]$ ($x = 0, 0.06, 0.09, 0.15$) further reveals that the strength of the enhanced signal in NH_4 libration and torsion modes are very sensitive to potassium concentration, and diminish quickly with small amount of potassium incorporation. At $x = 0.15$, the enhanced intensity vanishes, and the material has a collinear antiferromagnetic spin structure indicating the magnetic frustration is released due to potassium incorporation. The substitution of NH_4^+ with potassium breaks hydrogen bonds in the extended complex hydrogen-bonding network mediated through NH_4^+. Increasing potassium concentration corresponds to the instantaneous destruction of hydrogen bonds connecting neighboring Fe^{3+} ions. The fact that the magnetic structure switches to A-type antiferromagnetic for $x \geqslant 0.15$ indicates that the extended complex hydrogen-bonding network mediated through NH_4^+ is crucial in the enhanced magnetic frustration and the delicate balance between competing interactions responsible for the intriguing multiferroic properties in $(NH_4)_2[FeCl_5(H_2O)]$.

The fact that $(NH_4)_2[FeCl_5(H_2O)]$ remains paraelectric below the order-disorder transition at $T_s \approx 79$ K is very interesting. In ammonium compounds, a structural phase transition is often caused by the order-disorder transition of NH_4^+ ions. Because NH_4^+ motion often induces a structural transition, many ionic salts containing NH_4 are ferroelectric materials [46], and the incorporation of NH_4 has been used as a strategy to search for new multifunctional materials. In most cases, the incorporation of NH_4 results in type-I multiferroics, in which the ferroelectricity is induced at a high temperature associated with the structural transition and the ferroelectricity is decoupled with the magnetism as the magnetic order only sets in at a much lower temperature [47–49]. $(NH_4)_2[FeCl_5(H_2O)]$ is probably the first NH_4 based material exhibiting a type-II multiferroic behavior. The results from this study provide new insights into the crucial role NH_4^+ plays in emergent multiferroic phenomena in $(NH_4)_2[FeCl_5(H_2O)]$. The unique information opens a new door to go through in searching for new multifunctional materials by incorporation of NH_4 via a material-by-design approach.

[1] S. W. Cheong and M. Mostovoy, Multiferroics: a magnetic twist for ferroelectricity, Nat. Mater. **6**, 13 (2007).

[2] D. Khomskii, Classifying multiferroics: Mechanisms and effects, Physics **2**, 20 (2009).

[3] T. Kimura, T. Goto, H. Shintani, K. Ishizaka, T. Arima, and Y. Tokura, Magnetic control of ferroelectric polarization, Nature (London) **426**, 55 (2003).

[4] I. A. Sergienko and E. Dagotto, Role of the Dzyaloshinskii-Moriya interaction in multiferroic perovskites, Phys. Rev. B **73**, 094434 (2006).

[5] H. J. Xiang, S.-H. Wei, M.-H. Whangbo, and J. L. F. Da Silva, Spin-orbit coupling and ion displacements in multiferroic TbMnO₃, Phys. Rev. Lett. **101**, 037209 (2008).

[6] A. Malashevich and D. Vanderbilt, First principles study of improper ferroelectricity in TbMnO$_3$, Phys. Rev. Lett. **101**, 037210 (2008).

[7] I. V. Solovyev, Spin-spiral inhomogeneity as the origin of ferroelectric activity in orthorhombic manganites, Phys. Rev. B **83**, 054404 (2011).

[8] M. Kenzelmann, A. B. Harris, S. Jonas, C. Broholm, J. Schefer, S. B. Kim, C. L. Zhang, S.-W. Cheong, O. P. Vajk, and J. W. Lynn, Magnetic inversion symmetry breaking and ferroelectricity in TbMnO$_3$, Phys. Rev. Lett. **95**, 087206 (2005).

[9] S. W. Lovesey, V. Scagnoli, M. Garganourakis, S. M. Koohpayeh, C. Detlefs, and U. Staub, Melting of chiral order in terbium manganate (TbMnO$_3$) observed with resonant x-ray Bragg diffraction, J. Phys.: Condens. Matter **25**, 362202 (2013).

[10] K. Taniguchi, N. Abe, T. Takenobu, Y. Iwasa, and T. Arima, Ferroelectric polarization flop in a frustrated magnet MnWO$_4$ induced by a magnetic field, Phys. Rev. Lett. **97**, 097203 (2006).

[11] G. Lawes, A. B. Harris, T. Kimura, N. Rogado, R. J. Cava, A. Aharony, O. Entin-Wohlman, T. Yildrim, M. Kenzelmann, C. Broholm, and A. P. Ramirez, Magnetically driven ferroelectric order in Ni$_3$V$_2$O$_8$, Phys. Rev. Lett. **95**, 087205 (2005).

[12] R. Villarreal, G. Quirion, M. L. Plumer, M. Poirier, T. Usui, and T. Kimura, Magnetic phase diagram of CuO via high-resolution ultrasonic velocity measurements, Phys. Rev. Lett. **109**, 167206 (2012).

[13] H. J. Xiang and M.-H. Whangbo, Density-functional characterization of the multiferroicity in spin spiral chain cuprates, Phys. Rev. Lett. **99**, 257203 (2007).

[14] Y. J. Choi, H. T. Yi, S. Lee, Q. Huang, V. Kiryukhin, and S.-W. Cheong, Ferroelectricity in an ising chain magnet, Phys. Rev. Lett. **100**, 047601 (2008).

[15] M. Ackermann, D. Bruning, T. Lorenz, P. Becker, and L. Bohaty, Thermodynamic properties of the new multiferroic material (NH$_4$)$_2$[FeCl$_5$(H$_2$O)], New J. Phys. **15**, 123001 (2013).

[16] R. L. Carlin, S. N. Bhatia, and C. J. O'Connor, A new series of antiferromagnets, J. Am. Chem. Soc. **99**, 7728 (1977).

[17] J. N. McElearney and S. Merchant, Nonisomorphic antiferromagnetic behavior of two isomorphic salts: Low-temperature heat capacities and magnetic susceptibilities of (NH$_4$)$_2$FeCl$_5$ · H$_2$O and K$_2$FeCl$_5$ · H$_2$O, Inorg. Chem. **17**, 1207 (1978).

[18] M. Gabas, F. Palacio, J. Rodriguez-Carvajal, and D. Visser, Magnetic structures of the three-dimensional Heisenberg antiferromagnets K$_2$FeCl$_5$ · D$_2$O and Rb$_2$FeCl$_5$ · D$_2$O, J. Phys.: Condens. Matter **7**, 4725 (1995).

[19] J. Campo, J. Luzon, F. Palacio, G. J. McIntyre, A. Millan, and A. R. Wildes, Understanding magnetic interactions in the series A_2FeX_5 · H$_2$O (A = K, Rb; X = Cl, Br). II. Inelastic neutron scattering and DFT studies, Phys. Rev. B **78**, 054415 (2008).

[20] J. Alberto Rodríguez-Velamazán, O. Fabelo, A. Millan, J. Campo, R. D. Johnson, and L. Chapon, Magnetically-induced ferroelectricity in the (ND$_4$)$_2$[FeCl$_5$(D$_2$O)] molecular compound, Sci. Rep. **5**, 14475 (2015).

[21] W. Tian, H. Cao, J. Wang, F. Ye, M. Matsuda, J.-Q. Yan, Y. Liu, V. O. Garlea, H. K. Agrawal, B. C. Chakoumakos, B. C. Sales, R. S. Fishman, and J. A. Fernandez-Baca, Spin-lattice coupling mediated multiferroicity in (ND$_4$)$_2$FeCl$_5$ · D$_2$O, Phys. Rev. B **94**, 214405 (2016).

[22] Y. Wu, L. Ding, N. Su, Y. Ma, K. Zhai, X. Bai, B. C. Chakoumakos, Y. Sun, Y. Cheng, J. Cheng, W. Tian, and H.

Cao, Reentrance of spin-driven ferroelectricity through rotational tunneling of ammonium, arXiv:2101.02795.

[23] J. A. Rodríguez-Velamazán, O. Fabelo, J. Campo, Á. Millan, J. Rodriguez-Carvajal, and L. C. Chapon, Magnetic-field-induced change of magnetoelectric coupling in the hybrid multiferroic (ND$_4$)$_2$FeCl$_5$ · D$_2$O, Phys. Rev. B **95**, 174439 (2017).

[24] Y. Tokura, S. Seki, and N. Nagaosa, Multiferroics of spin origin, Rep. Prog. Phys. **77**, 076501 (2014).

[25] P. Toledano, N. Leo, D. D. Khalyavin, L. C. Chapon, T. Hoffmann, D. Meier, and M. Fiebig, Theory of high-temperature multiferroicity in cupric oxide, Phys. Rev. Lett. **106**, 257601 (2011).

[26] G. Giovannetti, S. Kumar, A. Stroppa, J. van den Brink, S. Picozzi, and J. Lorenzana, High-Tc Ferroelectricity Emerging from magnetic degeneracy in cupric oxide, Phys. Rev. Lett. **106**, 026401 (2011).

[27] G. Jin, K. Cao, G.-C. Guo, and L. He, Origin of ferroelectricity in high-Tc magnetic ferroelectric CuO, Phys. Rev. Lett. **108**, 187205 (2012).

[28] W. Tian, H. B. Cao, A. J. Clune, K. D. Hughey, T. Hong, J.-Q. Yan, H. K. Agrawal, J. Singleton, B. C. Sales, R. S. Fishman, J. L. Musfeldt, and J. A. Fernandez-Baca, Electronic phase separation and magnetic-field-induced phenomena in molecular multiferroic (ND$_4$)$_2$FeCl$_5$ · D$_2$O, Phys. Rev. B **98**, 054407 (2018).

[29] S. Biesenkamp, K. Schmalzl, P. Becker, L. Bohatý, and M. Braden, Multiferroic domain relaxation in (NH$_4$)$_2$[FeCl$_5$(H$_2$O)], Phys. Rev. B **108**, 094417 (2023).

[30] M. Ackermann, T. Lorenz, P. Becker, and L. Bohatý, Magnetoelectric properties of A$_2$[FeCl$_5$(H$_2$O)] with A = K, Rb, Cs, J. Phys.: Condens. Matter **26**, 506002 (2014).

[31] In modeling the magnetic spectrum measured from inelastic neutron scattering experiments using a linear spin wave theory, there is a sign difference between the Heisenberg Hamiltonian used for fitting the magnetic spectrum of K$_2$[FeCl$_5$(H$_2$O)] in Ref. [19] and for fitting the magnetic spectrum of (NH$_4$)$_2$[FeCl$_5$(H$_2$O)] in Ref. [32]. To be consistent, the minus signs were removed from the J values for K$_2$[FeCl$_5$(H$_2$O)] in Table I.

[32] X. Bai, R. S. Fishman, G. Sala, D. M. Pajerowski, V. O. Garlea, T. Hong, M. Lee, J. A. Fernandez-Baca, H. Cao, and W. Tian, Magnetic excitations of the hybrid multiferroic (ND$_4$)$_2$FeCl$_5$ · D$_2$O, Phys. Rev. B **103**, 224411 (2021).

[33] A. J. Clune, J. Nam, M. Lee, K. D. Hughey, W. Tian, J. Fernandez-Baca, R. S. Fishman, J. Singleton, J. H. Lee, and J. L. Musfeldt, Magnetic field-temperature phase diagram of multiferroic (NH$_4$)$_2$FeCl$_5$ · H$_2$O, npj Quantum Mater. **4**, 44 (2019).

[34] D. Brüning, T. Fröhlich, M. Langenbach, T. Leich, M. Meven, P. Becker, L. Bohatý, M. Grüninger, M. Braden, and T. Lorenz, Magnetoelectric coupling in the mixed erythrosiderite [(NH$_4$)$_{1-x}$K$_x$]$_2$[FeCl$_5$(H$_2$O)], Phys. Rev. B **102**, 054413 (2020).

[35] C. S. M. Partiti, H. R. Rechenberg, and J. P. Sanchez, The influence of NH$_4^+$ ionic motion on the magnetic structure of (NH$_4$)$_2$[FeCl$_5$(H$_2$O)]: A Mossbauer study, J. Phys. C: Solid State Phys. **21**, 5825 (1988).

[36] See Supplemental Material at http://link.aps.org/supplemental/10.1103/PhysRevB.110.064410 for the methods used to calculate and simulate the vibrational motion of NH$_4$ molecules; animations illustrating the motions of the NH$_4$ libration, NH$_4$

torsion, and water-wagging modes; and the enlarged regime of Fig. 3(a) between 0 meV and 15 meV.

[37] G. Kresse, and J. Furthmüller, Efficient iterative schemes for ab initio total-energy calculations using a plane-wave basis set, Phys. Rev. B **54**, 11169 (1996).

[38] P. E. Blöchl, Projector augmented-wave method, Phys. Rev. B **50**, 17953 (1994).

[39] G. Kresse, and D. Joubert, From ultrasoft pseudopotentials to the projector augmented-wave method, Phys. Rev. B **59**, 1758 (1999).

[40] J. P. Perdew, K. Burke, and M. Ernzerhof, Generalized gradient approximation made simple, Phys. Rev. Lett. **77**, 3865 (1996).

[41] J. Klimeš, D. R. Bowler, and A. Michaelides, Chemical accuracy for the van der Waals density functional, J. Phys.: Condens. Matter **22**, 022201 (2010).

[42] L. Wang, T. Maxisch, and G. Ceder, Oxidation energies of transition metal oxides within the GGA+U framework, Phys. Rev. B **73**, 195107 (2006).

[43] A. Togo and I. Tanaka, I. First principles phonon calculations in materials science, Scr. Mater. **108**, 1 (2015).

[44] Y. Q. Cheng, L. L. Daemen, A. I. Kolesnikov, and A. J. Ramirez-Cuesta, J. Chem. Theory Comput. **15**, 1974 (2019).

[45] Jmol: an open-source Java viewer for chemical structures in 3D, http://www.jmol.org/.

[46] A. H. Rama Rao, M. R. Srinivasan, H. L. Bhat, and P. S. Narayana, Dielectric behaviour and ferroelectricity in Alums, Ferroelectrics **21**, 433 (1978).

[47] R. Samantaray, R. J. Clark, E. S. Choi, and N. S. Dalal, Elucidating the mechanism of multiferroicity in $(NH_4)_3Cr(O_2)_4$ and its tailoring by alkali metal substitution, J. Am. Chem. Soc. **134**, 15953 (2012).

[48] G.-C. Xu, W. Zhang, X.-M. Ma, Y.-H. Chen, L. Zhang, H.-L. Cai, Z.-M. Wang, R.-G. Xiong, and S. Gao, Coexistence of magnetic and electric orderings in the metal–formate frameworks of $[NH_4][M(HCOO)_3]$, J. Am. Chem. Soc. **133**, 14948 (2011).

[49] R. Samantaray, R. J. Clark, E. S. Choi, H. Zhou, and N. S. Dalal, $M_{3-x}(NH_4)_xCrO_8$ (M = Na, K, Rb, Cs): A new family of Cr^{5+}-based magnetic ferroelectrics, J. Am. Chem. Soc. **133**, 3792 (2011).